The Co-adsorbent Effects of Nicotinic Acid and 1-Ethyl-3-Carboxypyridinium Iodide on the Performance of Dye-sensitized Solar Cells under Indoor Light Condition

Jui-Cheng Chang [1*, 2], Ming-Hsiang Tsai [3], Wen-Yueh Ho [4], I-Wen Sun [5], Tzi-Yi Wu [6*], Tsung-Lun Kan [7], and Yuh-Lang Lee [8*]

ABSTRACT

In this study, nicotinic acid (NTA) and its derivative, 1-ethyl-3-carboxypyridinium iodide ([ECP][I]), were utilized as co-adsorbents in the dye adsorption process of dye-sensitized solar cells (DSSCs). The co-adsorbent effects of the two molecules on the performance of DSSCs under indoor light illumination were investigated. The results showed that both the NTA and [ECP][I] significantly enhanced the short-circuit current density (Jsc), fill factor (FF), and output power relative to non-co-adsorbent device. Under the illumination of T5 light at an intensity of 200 lux, NTA (1.0 mM) showed 24.71 μAcm^{-2} in Jsc and 10.83 μWcm^{-2} in output power, and [ECP][I] (0.5 mM) displayed 23.80 μAcm^{-2} in Jsc and 10.33 μWcm^{-2} in output power. Also, using NTA, the output power value of the device was slightly higher than that obtained with chenodeoxycholic acid (CDCA). However, the performance by [ECP][I] is similar to the one that is commonly used in the literature. Both NTA and [ECP][I] could also be possibly used as co-adsorbents in dye-sensitized solar cells under indoor applications.

Keywords: Nicotinic acid, Dye-sensitized solar cell, Carboxypyridinium iodide, Co-adsorbent, Indoor lighting.

1. INTRODUCTION

Dye-sensitized solar cells (DSSCs) are considered as a new photovoltaic type with the characteristics of easy fabrication, low costs, and high performance. Three major parts are involved in a DSSC, including the photoelectrode, counter-electrode, and elec-

[1*] Project Assistant Professor (corresponding author), Department of Chemical and Materials Engineering, National Yunlin University of Science and Technology, Yunlin, Taiwan 64002, R.O.C. (e-mail: changjui@yuntech. edu.tw).

[2] Project Assistant Professor, Bachelor Program in Interdisciplinary Studies, National Yunlin University of Science and Technology, Yunlin, Taiwan 64002, R.O.C.

[3] Student, Department of Chemical Engineering, National Cheng Kung University (NCKU), Tainan, Taiwan 70101, R.O.C.

[4] Associate Professor, Department of Cosmetic Science, Chia Nan University of Pharmacy & Science, Tainan, Taiwan 71710, R.O.C.

[5] Professor, Department of Chemistry, National Cheng Kung University (NCKU), No. 1, University Rd., Tainan, Taiwan 70101, R.O.C.

[6*] Professor (corresponding author), Department of Chemical and Materials Engineering, National Yunlin University of Science and Technology, Douliou, Yunlin, Taiwan 64002, R.O.C. (email: wuty@yuntech. edu.tw)

[7] Student, Instrument Center, National Cheng Kung University (NCKU), Tainan, Taiwan 70101, R.O.C.

[8*] Professor (corresponding author), Department of Chemical Engineering, National Cheng Kung University (NCKU), Tainan, Taiwan 70101, R.O.C. (email: yllee@mail.ncku.edu.tw)

trolyte. Of these, the photoelectrode is regarded as a crucial factor in light harvesting from the environment because it helps transfer it into electrical energy. Grätzel and his co-workers proposed the first DSSC, based on nano-crystalline TiO_2. This DSSC can achieve a high efficiency of 12.3% and is potentially a cost-effective alternative to silicon-based photovoltaic technologies (Ling *et al*. 2013; Grätzel *et al*. 2001; O,Regan *et al*. 1991). A key component of DSSCs is the TiO_2 nanoparticle film, for it provides a high surface area to adsorb sensitizers (dye molecules) and also serves as the medium for electron transport. Therefore, the device performance relates to the charge transfer between the sensitizer and TiO_2 (Ling *et al*. 2013). Although the DSSCs are operated on light harvesting and the production of electron transferring, the charge separation and recombination pathways also often occur simultaneously at the TiO_2/dye/electrolyte interface. Although some methods have been considered to solve this inherent problem they still have disadvantages. For example, the development of high specific surface area (50 to 100 $m2g^{-1}$) of TiO_2 photoanodes can ensure enough dye absorption, but this method will also form much more surface interfaces to increase the possibility of charge recombination pathways between TiO_2 particles and I_3^- in the electrolyte (Wang *et al*. 2016; Zhang et al. 2007). Another strategy is the deposition of inorganic oxide particles (such as SnO_2, Al_2O_3, and Nb_2O_5) to modify the TiO_2 surface and form a thin insulating layer to inhibit the charge recombination (Kay *et al*. 2002; Son *et al*. 2015; Chen *et al*. 2001). However, the insulating layer is too thick so that this may reduce the charge injection efficiency. Therefore, much attention has been paid to organic molecules as they are commonly used as co-adsorbents on the TiO_2 surface in DSSCs.

A plethora of studies in relation to the use of co-adsorbents with organic molecules in dye-sensitized solar cells have been conducted in recent years (Wang *et al.* 2016; Shen *et al.* 2011; Han et al. 2012; Li *et al.* 2014; Lim *et al.* 2011; Song *et al.* 2011; Silva *et al.* 2019; Huang *et al.* 2019). The purpose of co-adsorbents is to reduce the possible charge recombination pathways occurring at the TiO_2/dye/electrolyte interface. An ideal candidate for a co-adsorbent should have the three following main characteristics: (i) it should have a large molar extinction coefficient in the infrared region or around 400 nm to recover the dip in the IPCE spectra induced by I_3^-; (ii) the structure of the molecule should suitably avoid competitive adsorption among dyes and effectively suppress the aggregation of dyes on the TiO_2 surface; and (iii) it should be able to reduce the recombination of electrons in the TiO_2 film with I_3^- and other acceptor species by the formation of a compacted molecule monolayer covering the bare TiO_2 surface (Han *et al.* 2012). Several kinds of organic molecular co-adsorbents, such as decylphosophnic acid (DPA), dineohexylbis (3.3-dimethyl) phosphinic acid (DINHOP), and chenodeoxycholic acid (CDCA), have been examined to modify the TiO_2-dye interface in DSSCs, including phosphonic acids and carboxylic acids (Song *et al.* 2011). These co-adsorbents bind to the TiO_2 surface through phosphonate and carboxylate ester bonds, respectively. As documented in the literature, CDCA co-adsorbent is the most commonly used one in DSSCs because it has a good capability to reduce the dye aggregation (Chandiran *et al.* 2017; Lee *et al.* 2013). Yet, using these co-adsorbents, with particular reference to stearic acid, can typically reduce the amount of dye-loading on the surface of TiO_2 because the big stearic acid molecules are able to compete with the dye or hinder the dye anchoring on the TiO_2 surface. The CDCA also has some disadvantages, such as being difficult to synthesize and very expensive. Therefore, very few studies in relation to the application of DSSCs, using small molecules as co-adsorbents, have been developed (Nguyen *et al.* 2017). Besides, 4-tert-Butylpyridine (4-TBP), a relatively small molecule, is currently used as the most popular additive. This small molecule has been introduced into DSSCs electrolyte to increase the open-circuit voltage (Voc) of DSSCs. The increase in Voc may be due to the fact that 4-TBP adsorbs on the TiO_2 surface and causes a negative shift of the Fermi level. However, the 4-TBP cannot completely coordinate titanium atoms on the TiO_2 surface (form Ti ← N coordination bonds), thereby causing the possibility of back electron transfer. Accordingly, a compound similar to 4-TBP needs to be found and used as a co-adsorbent in DSSCs to form covalent bonds with the surface of TiO_2. Nicotinic acid (NTA) considered similar to 4-TBP is an inexpensive compound. It contains a carboxylic group bound to a pyridine ring and has been chosen as a suitable co-adsorbent. NTA can form ester bonds with hydroxyl groups on the TiO2 surface. This results in a 50% positive enhancement of the performance of DSSCs. The NTA cannot compete with dye at the optimum concentration of 1Mm because its concentration is more than that of the other co-adsorbents (CDA: 30 µM; OPA: 15 µM) (Nguyen *et al.* 2017). Another possible small molecule is [ECP][I], the derivation of NTA. In 2011, Prof. Ho reported that [ECP][I] could be used as a co-adsorbent for DSSCs under one sun condition. The use of [ECP][I] led to a 20% overall improvement in efficiency, compared to a non-co-adsorbent device (in an N719 dye system, 8 µm TiO_2). This was due to electron-donating and the abundant concentration of I^-. The concentration of such can influence the interaction with the TiO_2 electrode and so cause the conduction band (CB) edge of TiO_2 to shift to a more negative potential (Chang *et al.* 2011). In this study, both of the small molecules of [ECP][I] and NTA were still used, and yet they were performed under indoor lighting conditions.

Indoor light energy is viewed as an abundant source because of its various applications. For example, solar cells are used to convert the radiant energy to electricity. This field of research has become highly important because this leads to the direction of development for emerging photovoltaic (PV) devices, such as dye-sensitized, perovskite, and organic thin-film solar cells (Chen *et al.* 2017; Mathews *et al.* 2016). Indoor light intensity levels are a factor of ~10^4 less than the 1000 Wm^{-2} intensity of one sun standard test conditions (STC). Based on a review of the previous literature, DSSCs have the advantage of harvesting the indoor light and converting it into electricity, and thus many related studies have been conducted to examine DSSC applications associated with indoor lighting conditions in recent years. For example, the DSSCs can be potentially applied for the Internet of Things (IoT). That is because the necessary interconnected devices and wireless sensor nodes mainly need the optimal energy-harvesting systems to provide power autonomy and start up. Some studies have found that the efficiency of harvesting indoor lighting with DSSCs (2.92 μWcm^{-2}) is better than that obtained with other types of solar cell, such as poly-crystalline silicon (poly-Si, 2.85 μWcm^{-2}) and amorphous silicon (a-Si, 0.67 μWcm^{-2}) solar cells under 200lux illumination from a compact fluorescent lamp (Rossi *et al.* 2015; Freitag *et al.* 2017). Since [ECP][I] and NTA are continuously used as co-adsorbents in DSSC applications under indoor lighting, t has also been proved to enable [ECP][I] and NTA manifest good performance in this study.

2. MATERIALS AND METHODS

2.1 Chemicals

Pyridine-3-carboxylic acid (Nicotinic acid), ethyl iodide, Dimethyl sulfoxide (DMSO), 4-*tert*-butylpyridine (TBP), Guanidinium thiocyanate (GuSCN), sodium hydroxide and iodine were purchased from Sigma-Aldrich. Besides, acetonitrile (AN), ethanol (EtOH), and tert-butanol (t-BuOH) were purchased from J.T. Baker. Next, 1,3-dimethylimidazolium iodide ([DMI][I]) was purchased from TCI. Also, titanium dioxide paste with particles size 30 nm and 400 nm was sold by Dyesol and CCIC (Catalysts & Chemicals Industries Co., Ltd) respectively. Meanwhile, cis-bis (isothiocyanato) (2,2-bipyridyl-4,4-dicarboxylato) (4,4-di-nonyl-2,2-bipyridyl) ruthenium (II) (Z907) was sold by Solaronix. More importantly, all chemicals were used without further purification, and The electrolyte was comprised of the following main components, including 0.2M [DMI][I] + 0.01M I_2 + 0.8M TBP + 0.1M GuSCN in a mixture of 3-methoxypropionitrile (MPN). Finally, this aforesaid electrolyte was used in this current study.

2.2 Characterization of structure and properties of 1-ethyl-3-carboxypyridinium iodide [ECP][I]

The ^1H spectra of the purified products [ECP][I] were recorded in DMSO-d6 (Cambridge Isotope Laboratories Inc., 99.9%D) on a Bruker Avance 500 spectrometer at 25 °C. The fragment molecular weight of cations and anions in [ECP][I]

were obtained, using a mass spectrometer (model: LTQ Orbitrap XL, Thermo-Fisher, American), and the determination of functional group was obtained, using FT-IR spectra (model: Nicolet 6700, Thermo Electron Corporation, American).

The synthesis route for [ECP][I] is given in Scheme 1 (Chang *et al.* 2011). The ^{1}H NMR (shown in Figure S1a), ^{13}C NMR (Figure S1b), and mass spectra (Figure S2a and S2b) of [ECP][I] are summarized as follows: 1H NMR (500MHz, DMSO-d_6): δ 9.56 (s, 1H), 9.31 (d, J = 6.1 Hz, 1H), 8.94 (d, J = 7.8 Hz, 1H), 8.27 (dd, J= 7.8, 6.1 Hz, 1H), 4.74 (q, J = 7.3 Hz, 2H), 1.57 (t, J = 7.3 Hz, 3H). 1H NMR (125MHz, DMSO-d^6): δ 163.1, 147.2, 145.8, 145.1, 131.1, 128.3, 56.7, 16.3. LRMS-ESI (+ve): m/z [M-I⁻]$^+$ calcd for $C_8H_{10}NO_2^+$: 152.0706; found: 152.0706. LRMS-ESI (-ve): m/z calcd for [I]-: 126.9050; found: 126.9055.

2.3   Preparation of photoelectrode

The fluorine-doped tin oxide (FTO) substrate was washed and sonicated with water, neutral detergent, and acetone. Then, this FTO substrate was immersed into 40 mM $TiCl_4$, subjected to the pretreatment conditions (in a 70 °C oven for 30 min), and rinsed with water and ethanol to better form the dense precursor of titanium dioxide (TiO_2). The TiO_2 pastes were coated on the pretreated FTO with an active area of 0.16 cm^2 by the screen-printing method. 6 μm thicknesses-dyesol and 4 μm thicknesses-CCIC TiO_2 pastes were used in the main and light-scattering layers, respectively. After this, the sample underwent sintering under airflow at 150 °C for 15 min, 325 °C for 5 min, 450 °C for 5 min, and 500 °C for 30 min to finish the TiO_2 electrode. These electrodes were immersed into $TiCl_4$ solution. They were sonicated for 15 min, rinsed with ethanol, and dried at 70 °C oven 30 min. The TiO_2 electrodes were then disinfected by UV-ozone, heated at 470 °C for 30 min to decompose the aliphatic hydrocarbons, and finally cooled down to around 100 °C. Next they were immersed into a dye solution mixed with 0.5 mM Z907 and different co-adsorption ratios (0.1, 0.2, 0.5, 1, and 2 mM for NTA or [ECP][I]) in dimethyl sulfoxide (DMSO) / tert-butanol (t-BuOH) / acetonitrile (AN) (1:4.5:4.5 in volume). The TiO_2 electrodes were immersed in this solution and kept at 25 °C for 6 hours. This enabled the dye to adsorb onto the TiO_2 surface, which was followed by rinsing in ethanol and drying in air.

2.4   Cell assembly and measurements

Holes were drilled in the counter electrode and then a layer of platinum was sputtered on the FTO glass (called a Pt-sputtered FTO). The Pt-sputtered FTO and the dye-sensitized photoelectrode with co-adsorbent were sandwiched, using a 30um thick spacer. The electrolyte was injected and penetrated into the cell from two holes on the back of counter electrode. Finally, the two holes were sealed with a 60um surlyn film covered with a thin glass slide under heat (210°C). The photovoltaic performance, the current-voltage (I-V) characteristics under a Philips T5 fluorescence lamp surrounded by black cloth to avoid the light diffusion, was analyzed by a Keithley 2420 sourcemeter. The spectra-mismatch factor of the intensity of indoor lighting was corrected by a SOMA spectra analyzer (model: S-2440). The incident photon-to-current conversion efficiency (IPCE) of the cells was measured by means of appropriate equipment (model: QE-R3011, Enil Technology Co., Ltd. Taiwan). Electrochemi-

cal impedance spectroscopy (EIS) measurements of the cells were carried out, using Autolab ECO Chemie PGSTAT 30 in the frequency range from 10^5 Hz to 5 × 10^{-2} Hz at a potential modulation of 10 mV (in dark conditions). The resulting impedance data were fitted with Z-view software to better collect the resistance of recombination (R_{ct}), interfacial resistance between electrolyte and Pt-sputtered FTO (R_{pt}), electron lifetime, and electron density.

2.5   UV-Visible absorption measurements

In order to calculate the amount of dye loaded onto the TiO_2 films, the molar absorption coefficient of Z907 dye must be first obtained by UV-Vis spectrophotometry (model: U-4100, Hitachi, Japan). The linear equation is fitted by the absorbance of five different concentrations in Z907 dye (0.01 mM to 0.05 mM) to obtain the molar absorption coefficient. Then, the dye-sensitized photoanodes with free dye as a reference and different ratios of co-adsorbent were immersed into 2 mL of 0.1M NaOH solution (solvent: H_2O / DMSO / EtOH = 3 / 3 / 4 in volume) overnight. This was followed by the measurement of the absorbance of the resulting solution to obtain the dye loading (from the linear equation by using a UV-Vis spectrophotometer).

2.6   FTIR measurements

In addition to characterizing the functional groups of NTA and [ECP][I], FTIR can also be used to examine the co-adsorbent caused to form on the surface of the TiO_2 films. Spectra were obtained with 32 scans. The TiO_2 films (12 μm) were immersed into 20 mM co-adsorbent (NTA and [ECP][I], respectively) solution for 12 hours. They were left dry in air, and finally scratched to characterize the functional group of co-adsorbent based on the TiO_2 films.

3.   RESULTS AND DISCUSSION

3.1   Characterization of pyridinium molten salt with nicotinic acid moiety [ECP][I]

Nicotinic acid (NTA) is widely available on the market; however, the [ECP][I] must be synthesized from NTA precursor. The structure of [ECP][I] is given in Scheme 1 (Chang *et al.* 2011). The molten salt [ECP][I] was prepared by quaternization reactions of NTA as a nucleophile with two equimolar amounts of 1-iodoethane. This was to conduct the S_N2 substitution reaction at 110 °C in acetonitrile. The difference in functional groups between the NTA and the [ECP][I] was measured by FT-IR, with the spectrum illustrated in Fig. 1. The [ECP][I] showed the obvious C-H bond stretching (2937 and 2982 cm^{-1}) and C-H bondbending (1381, 1447, and 1480 cm^{-1}) different from those obtained with NTA. In order to determine the co-adsorbent caused to form on TiO_2 film, the TiO_2 films were immersed in co-adsorbent solutions (20 mM NTA or [ECP][I], the solvent system: DMSO / t-BuOH / ACN = 1: 4.5: 4.5 in volume) without the effect of Z907 dye. After the TiO_2 films were immersed, the color changed from white to yellow due to adsorption of [ECP][I], but the one in NTA still remained white, as shown in Fig. 2. The transmittance bands of TiO_2 powders with co-adsorbents (called TiO_2@NTA or TiO_2@[ECP][I]) are summarized in Figs 3a, 3b, and Table S1. As shown in Table S1, both the TiO_2@NTA and TiO_2@[ECP][I] demonstrated
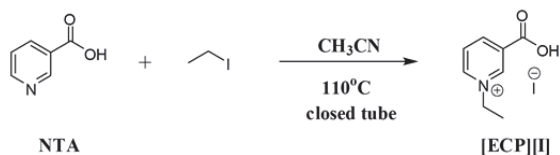
Scheme 1   The synthesis route of [ECP][I]
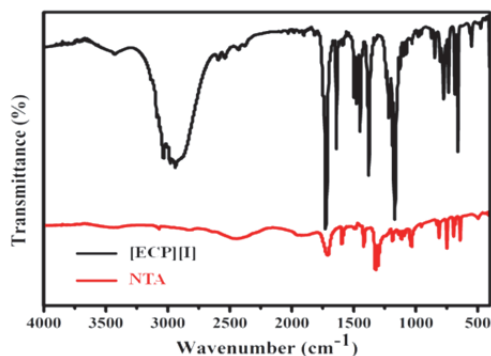
Fig. 1   The infrared spectrum of [ECP][I] and NTA
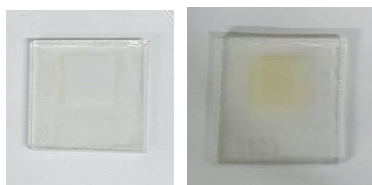
Fig. 2   The status of TiO$_2$ films after being immersed in NTA (left, white) and [ECP][I] (right, yellow)
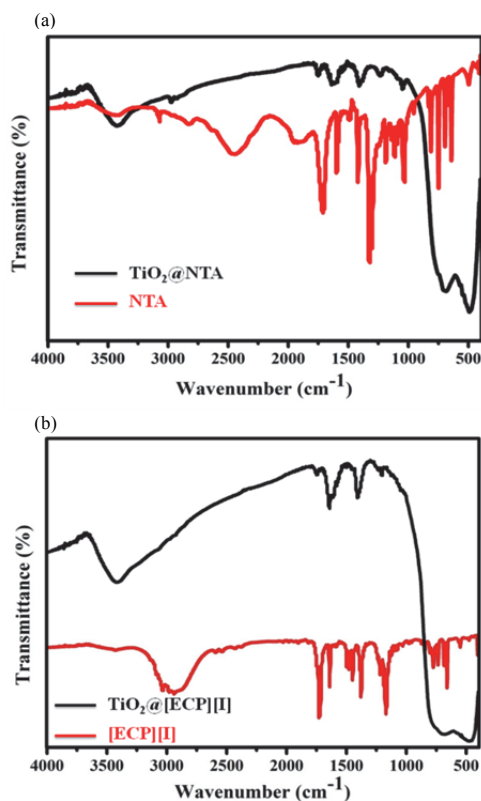
Fig. 3   The infrared spectrum of (a) TiO$_2$@NTA and (b) TiO$_2$@[ECP][I] (The peaks of NTA and [ECP][I] are the references, respectively)

some similar bands as molecular NTA and [ECP][I], respectively. The new peak observed at 1045 and 1050 cm^{-1} was related to the stretching vibration of C-O-Ti of TiO$_2$@NTA and TiO$_2$@[ECP][I] in the FT-IR spectrum, respectively. This new peak suggests that the two co-adsorbents are successfully bound to the surface of TiO$_2$ electrodes via the carboxylic acid group.

3.2   Solar cell performance under indoor application

In this study, the two compounds were used for DSSCs under indoor lighting conditions. Table 1 depicts the details of the photovoltaic performance, *e.g.*, open-circuit potential (Voc), short-circuit current density (Jsc), fill factor (FF), output power, and dye-loading values with different ratios of co-adsorbents. The I-V curves with their focus on the high output power condition (devices D, I, and J) included references (device A: dye alone; and L: CDCA co-adsorbent), as shown in Fig. 4. By referring to Table 1 and Fig. 4, some of the results can be described, and they are now provided below. (i) The two co-adsorbents enhanced the Jsc significantly but not the Voc. Devices D and J had high output power with the [ECP][I] and NTA systems, respectively. The NTA system had greater improvement of Jsc and output power than [ECP][I]. At the same concentration (0.5 mM), NTA had 10.8% improvement in Jsc and 12.1% in output power, but the [ECP][I] had 6.7% in Jsc and 6.9% in output power. (ii) The dye-loading of the NTA system was higher than that of the [ECP][I] system. (iii) The output power of NTA was slightly higher than that of CDCA (40 mM, device L) in 0.5 mM, 1.0 mM, and 2.0 mM conditions. However, the output power of [ECP][I] (in 0.5 mM) was slightly lower than that of CDCA. Based on this part of the results, whether in the NTA or [ECP][I] system, the concentrations of co-adsorbents needed are significantly lower than those obtained with CDCA. Both the NTA and the [ECP][I] molecules thus have the potential to replace the frequently-used CDCA (Chandiran *et al*. 2017; Lee *et al*. 2013). The trend of the output power may have a relationship with the structure of the co-adsorbents. The literature on the co-adsorbents applied for one sun conditions show that their dipole moments are the key factor in increasing Voc (Kusama *et al*. 2013; Zhang *et al*. 2005). Prof. Kusama found that the pyrimidine molecule additive has the N atoms needed to increase the dipole moment and improve Voc. The pyrimidine groups also have electron donicity and so produce a lot of iodide anions and increase the Voc of the cell. The research carried out by M. Grätzel's group also suggests the dipole moment when 4-guanidinobutyic acid (4-GBA) is served as a co-adsorbent can influence the Voc in one sun condition. In this study, the NTA that has N atoms also showed slight improvement in Voc, even with indoor lighting. The Z907 and co-adsorbents (NTA or [ECP][I]) adsorbed on the TiO$_2$ were completely desorbed by soaking dyed photoanodes in aqueous solutions of 0.1M NaOH (solvent: H$_2$O / DMSO / EtOH = 3 / 3 / 4) overnight. Figure S3a presents the absorption spectra of pure Z907 dye with five concentrations (0.01 mM to 0.05 mM). Then, these absorption values of five concentrations were fitted, using a linear equation to obtain the molar absorption coefficient (shown in Fig. S3b). Figure S3c shows the absorption spectra of desorbed solutions (devices A, D, I, J, and L, respectively), and these absorbances could be into a fitted linear equation to obtain the value of dye-loading. As indicated in Table 1, the high output power in the NTA system was associated with low dye-loading. In the [ECP][I] system, an increase in concentration resulted in a decrease in dye

loading. As shown in Fig. S3c, low dye loading was accompanied by low absorbance of the UV-Vis spectra, and this also indicated an effective reduction in molecular dye aggregation. Generally, relatively high dye loading leads to more light harvesting and so can enhance the photocurrent of DSSCs, but the co-adsorbents will affect the loading amount and competitive adsorption with dyes. In the indoor lighting condition, the yellowish solid [ECP][I] may compete with the dye for adsorption onto TiO$_2$ films, thus leading to less output power, especially in the high concentration condition.

In order to further discuss the enhancement of Jsc, the incident photon-to-electron conversion efficiency (IPCE) must be measured in this study. IPCE as a function of wavelength was measured to better evaluate the photo-response of the photoelectrodes in the whole spectral region. Figure 5 shows the IPCE spectra for TiO$_2$ films before and after the co-adsorption with NTA, [ECP][I], and CDCA, respectively. Upon addition of NTA, [ECP][I], or CDCA in the Z907 dye solution, IPCE obviously increased at 530 nm. The maximum IPCE increased from 65% (device A) to 70% when 1.0 mM NTA (device J) was added to the Z907 dye solution. Also, this IPCE increased to 69% with 0.5 mM [ECP][I] (device D) in the Z907 dye solution. CDCA with approximately 70% IPCE was similar to NTA (1.0 mM) and [ECP][I] (0.5 mM). Figure 5 also demonstrates that both the NTA and [ECP][I] had good light harvesting effects at the region from 350 nm to 650 nm. For device A, from 350 nm to 650 nm, the IPCE value was relatively low. When NTA and [ECP][I] were introduced as the co-adsorbents for devices D, I, and J, the absorption of 350 nm to 650nm dramatically increased. This means that the presence of the co-adsorbent not only reduces the dye aggregation for satisfactory absorption ability of the devices, but also effectively reflects the light from 350 nm to 650 nm, and hence enhances the light harvesting ability of TiO$_2$ photoanodes for a better photo-response. Thus, the IPCE has three positive correlation effects: the efficiency of light harvesting in the device, electron injection to the conduction band of TiO$_2$, and electron collection. In this study, the main reason for this might have been due to the electron injection. In the report of Prof. Shi (Hou *et al.* 2015), the acetyl acetone-type co-adsorbent with the aromatic group has a good ability of electron donation to not only enhance the electron injection but also increase the Jsc under illumination of AM 1.5G (intensity = 100 mWcm^2). Besides, even when used under indoor lighting condition, the good performance of NTA and [ECP][I] may also be ascribed to the fact that they are aromatic structures, thus increasing Jsc.

The effect of co-adsorbents adsorbed onto TiO$_2$ films was also reflected in the dark current, which results from the reduction of tri-iodide by the conduction band electrons of TiO$_2$. This is considered crucial to the properties of the cells, for it reveals the situation in relation to the surface statement and energy level of TiO$_2$. As can be seen from Fig. 6, the co-adsorbents of NTA (0.5 mM, device I) and CDCA (40.0 mm, device L) had identical effects, and this was observed to be slightly higher than that of Z907. The co-adsorbents as such only served to retard recombination, when compared to the [ECP][I] system. That was because the [ECP][I] system increases the charge recombination. This might have been also related to the structure of [ECP][I] and NTA. Based on these aforesaid results, NTA and [ECP][I] could possibly contribute to the significantly increased photocurrent of the DSSCs instead of Voc.

Electrochemical impedance spectra (EIS) were further used to reveal the effects of NTA and [ECP][I] on the interfa-

cial resistance and electron life time before recombination. Figure 7a shows Nyquist plots of electrochemical impedance spectra measured in the dark condition with an identical forward bias of −0.70V. Nyquist plots generally consist of three semicircles. The leftmost semicircle reveals that the redox charge transfer at the platinum counter electrode occurs at high frequencies. The middle semicircle at intermediate frequencies is recombination at the TiO$_2$/electrolyte interface. This recombination resistance can be read through the diameter. The rightmost semicircle at low frequencies reflects ion diffusion in the electrolyte, but this rightmost semicircle often is overlapped with the mid-frequency semicircle. In this study, the cell gap was no larger than 30 μm, which means that the diffusion resistance of iodide and tri-iodide within the electrolyte was quite small, and thus the rightmost semicircle in this study could not be measured. The experimental EIS data could be fitted to obtain the values of recombination resistance (R$_{ct}$) and charge transfer resistance (R$_{pt}$) at the platinum counter electrode/electrolyte interface, and these values are summarized in Table 2. As indicated in Fig. 7a and Table 2, the co-adsorbent CDCA (device L) had the largest second semicircle, and this means that the recombination resistance (R$_{ct}$) increased to depress the recombination. The co-adsorbent NTA (0.5 mM, device I) had a larger second semicircle than Z907 only (device A), but the second semicircle of [ECP][I] (0.5 mM, device D) was smaller than that of Z907 only. This part of the results indicates that the [ECP][I] system could not effectively depress the recombination. Meanwhile, these results also showed the performance of electron life time. As indicated in Table 2, the electron life time of NTA (0.5 mM) was also higher than Z907 only, and this result demonstrates that the use of the co-adsorbent NTA could effectively prevent electron recombination from the oxidized I3- in the electrolyte and thus achieved a longer electron life time, leading to better device performance. However, as indicated in Fig. 7b, both the [ECP][I] (0.5 mM) and NTA (0.5 mM) had relatively small leftmost semicircles, when compared to Z907 only and co-adsorbent CDCA. This also suggests that the [ECP][I] (0.5 mM) and NTA (0.5 mM) made the charge transfer from the platinum counter electrode/electrolyte interface faster, and that this factor possibly contributed to the increase in Jsc. Besides, the chemical capacitance was obtained as well by fitting the experimental data of some devices (devices A, D, I, J, and L) with an equivalent circuit. Figure 8a shows the chemical capacitance of these five devices under different applied bias voltages. Devices I and L had relatively low capacitance values. The results indicate that the conduction band of the TiO$_2$ negatively shifted and the Voc increased when treated with NTA (0.5 mM) and CDCA (40 mM). The charge recombination resistance (R$_{ct}$) at the interface between and electrolyte redox species was further investigated from EIS. Comparing these five devices, devices I and L showed the largest value at any given bias voltage, as presented in Fig. 8b. This figure also shows that device D (0.5 mM [ECP][I]) had a lower Rct value than device A (Z907 only). The electron lifetime, which can be calculated from the chemical capacitance multiplied by Rct in fitting the EIS curves, is plotted in Fig. 8c. NTA also exhibited enhanced electron lifetimes in these five Z907 based DSSC devices, while [ECP][I] exhibited the lowest electron lifetime. Overall, the EIS results suggest that the use of NTA as a co-adsorbent grafted with Z907 dye is more effective than [ECP][I] in suppressing the recombination of electrons, which results in improved Voc to occur. In the above-mentioned solar cell performance in indoor light-

ing condition, NTA and [ECP][I] could both contribute to the increased photocurrent. The structures of NTA and [ECP][I] may be the essential factor in this study, although a more detailed discussion of this and the related effects would require more careful and comprehensive research.
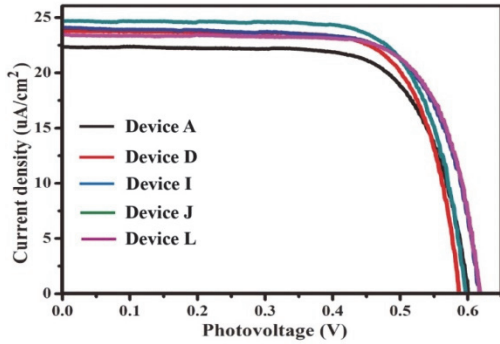
Fig. 4   Representative photocurrent density-voltage curves for DSSCs sensitized with Z907 alone (device A) and Z907 combined with co-adsorbents in varying concentrations (device D: 0.5 mM [ECP][I]; device I: 0.5 mM NTA; device J: 1.0 mM NTA; and device L: 40.0 mm CDCA), under indoor lighting condition. The active area is 0.16 cm^2.
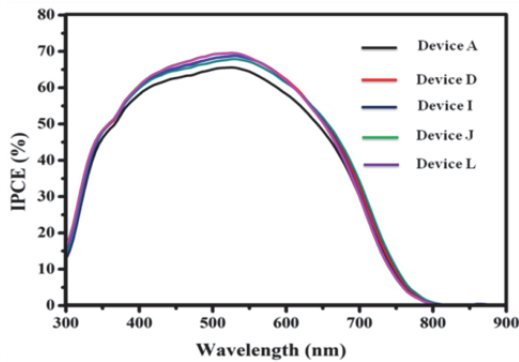
Fig. 5   IPCE spectra of devices A, D, I, J, and L with different concentrations of NTA, [ECP][I], and CDCA (device D: 0.5 mM [ECP][I]; device I: 0.5 mM NTA; device J: 1.0 mM NTA; and device L: 40.0 mM CDCA. The spectra for device D are similar to those for device L).
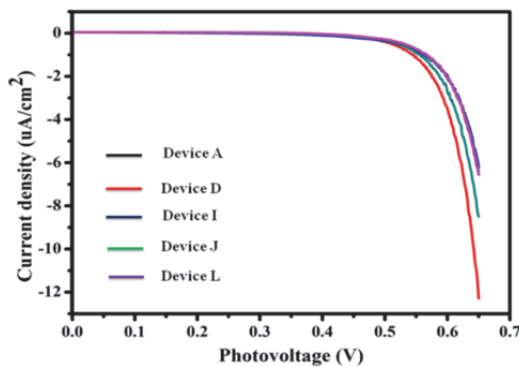
Fig. 6   Current density-voltage characteristics of devices fabricated with TiO$_2$ film stained with Z907 only (device A), Z907/[ECP][I] (0.5 mM, device D), Z907/NTA (0.5 mM, device I; and 1.0 mM, device J), or Z907/CDCA (40.0 mM, device L) under indoor lighting condition in the dark (device A is similar to devices I and L).
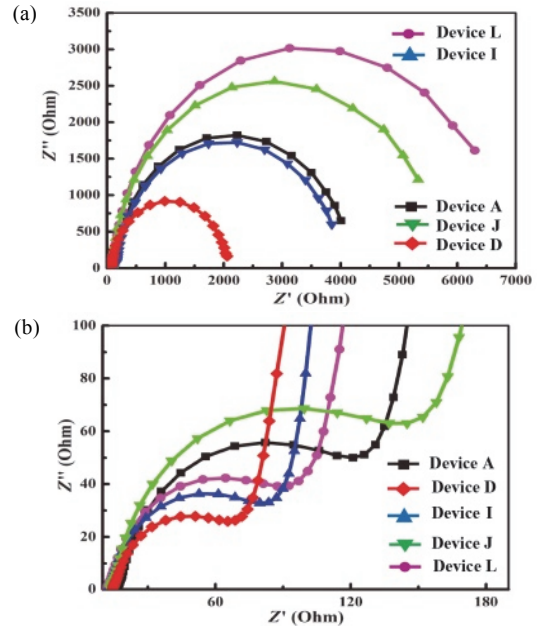
Fig. 7   (a) The Nyquist plots of EIS spectra and (b) rightmost semicircles (Rpt) are measured for devices (A, D, I, J, and L) at an external potential of -0.70V in the dark.
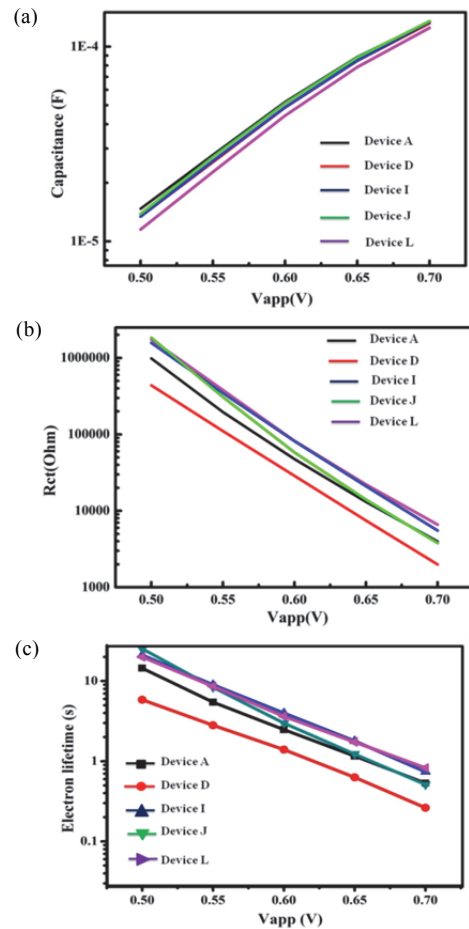
Fig. 8   Electrochemical parameters of DSSCs (devices A, D, I, J, and L) measured at different forward biases near their open-circuit potentials in the dark. (a) Chemical capacitance, (b) recombination resistance Rct, and (c) electron lifetime.

Table 1 **The photovoltaic performance of DSSCs based on co-adsorbent NTA and [ECP][I] with different concentrations under indoor lighting condition.**

Device	Co-adsorbent	J_{sc} (μAcm^{-2})	V_{oc} (mV)	FF	Output power ($\mu W/cm^2$)	Dye-loading ($\times 10^{-9}$ mloe/cm^2)
A	-	22.30	0.601	0.719	9.66	1.89
B	0.1 mM [ECP][I]	22.70	0.590	0.724	9.70	2.25
C	0.2 mM [ECP][I]	22.98	0.593	0.738	10.07	1.79
D	0.5 mM [ECP][I]	23.80	0.587	0.739	10.33	1.53
E	1.0 mM [ECP][I]	22.15	0.598	0.738	9.78	1.33
F	2.0 mM [ECP][I]	21.19	0.603	0.734	9.38	1.45
G	0.1 mM NTA	23.30	0.605	0.722	10.20	2.30
H	0.2 mM NTA	23.20	0.608	0.730	10.31	2.10
I	0.5 mM NTA	24.10	0.617	0.719	10.68	1.73
J	1.0 mM NTA	24.71	0.597	0.734	10.83	1.88
K	2.0 mM NTA	24.48	0.600	0.738	10.84	2.10
L	40.0 mM CDCA	23.47	0.617	0.736	10.67	1.59

Table 2 **The EIS results (Rpt and Rct) and electron lifetime before the recombination for devices (A, D, I, J, and L) at −0.70V in the dark.**

Device	Co-adsorbent	R_{pt} (Ohm)	R_{ct} (Ohm)	Electron lifetime (s)
A	-	132.73	3978	0.53
D	0.5mM [ECP][I]	68.81	1987	0.26
I	0.5mM NTA	86.28	5530	0.74
J	1.0mM NTA	164.45	3787	0.51
L	40.0mM CDCA	102.54	6593	0.82

4. CONCLUSIONS

The results of this current experimental study showed that the total PCE was significantly improved in indoor lighting condition by introducing NTA and [ECP][I] into Z907 system DSSCs. The infrared spectrum showed that the co-adsorbents (NTA and [ECP][I]) successfully adsorbed onto TiO$_2$ film. In terms of the solar performance in the condition of indoor lighting, both the NTA and [ECP][I] showed an improvement in Jsc to enhance the output power. In 0.5mM, NTA had 10.8% improvement in Jsc and 12.1% in output power, and the [ECP][I] had 6.7% in Jsc and 6.9% in output power relative to the reference dye only device. The NTA also showed a slight improvement in Voc to suppress the charge recombination. The output power of NTA and [ECP][I] also suggests that they had good potential to replace CDCA as novel co-adsorbents in dye-sensitized solar cells with indoor applications. These results might have been attributed to some factors, such as electron donicity of N atoms, molecular dipole moment, and phenyl fragment. However, future studies in relation to these aforesaid factors should be conducted in detail to confirm whether this is the case or not.

SUPPORTING INFORMATION AVAILABLE

The ^{1}H, ^{13}C, and DEPT-135 NMR spectra of the [ECP][I] are presented in Fig. S1. The Mass spectrums of cation and anion of the [ECP][I] are illustrated in Fig. S2. Table S1 summarizes the FT-IR signals of NTA, [ECP][I], TiO$_2$@NTA, and TiO$_2$@[ECP][I]. Figure S3 depicts the equation of dye-loadong calculation.

REFERENCES

Chandiran, A.K., Zakeeruddin, S.M., Humphry-Baker, R., Nazeeruddin, M.K., Grätzel, M., and Sauvage, F. (2017). "Investigation on the Interface Modification of TiO$_2$ Surfaces by Functional Co-Adsorbents for High-Efficiency Dye-Sensitized Solar Cells." *ChemPhysChem*, **18**, 2724-2731.

Chang, J.C., Yang, C.H., Yang, H.H., Hsueh, M.L., Ho, W.Y., Chang, J.Y., and Sun, I.W. (2011). "Pyridinium molten salts as co-adsorbents in dye-sensitized solar cells." *Solar Energy*, **85**, 174-179.

Chen, C.Y., Jian, Z.H., Huang, S.H., Lee, K.M., *et al.* (2017). "Performance Characterization of Dye-Sensitized Photovoltaics under Indoor Lighting." *The Journal of Physical Chemistry Letters*, **8**, 1824-1830.

Chen, S.G., Chappel, S., Diamant, Y., and Zaban, A. (2001). "Preparation of Nb$_2$O$_5$ Coated TiO$_2$ Nanoporous Electrodes and Their Application in Dye-Sensitized Solar Cells." *Chemistry of Materials*, **13**, 4629-4634.

DeRossi, F., Pontecorvo, T., and Brown, T.M. (2015). "Characterization of photovoltaic devices for indoor light harvesting and customization of flexible dye solar cells to deliver superior efficiency under artificial lighting." *Applied Energy*, **156**, 413-422.

Freitag, M., Teuscher, J., Saygili, Y., Zhang, X., Giordano, F., Liska, P., Hua, J., Zakeeruddin, S.M., Moser, J., Grätzel, M., and Hagfeldt, A. (2017). "Dye-sensitized solar cells for efficient power generation under ambient lighting." *Nat Photon*, **11**, 372-378.

Grätzel, M. (2001). "Photoelectrochemical cells." *Nature*, **414**, 338-344.

Han, L., Islam, A., Chen, H., Malapaka, C., Chiranjeevi, B., Zhang, S., Yang, X., amd Yanagida, M. (2012). "High-efficiency dye-sensitized solar cell with a novel co-adsorbent." *Energy & Environmental Science*, **5**, 6057-6060.

Hou, R., Yuan, S., Ren, X., Zhao, Y., Wang, Z., Zhang, M., Li, D., and Shi, L. (2015). "Effects of acetyl acetone-typed co-adsorbents on the interface charge recombination in dye-sensitized solar cell photoanodes." *Electrochimica Acta*, **154**, 190-196.

Huang, G.W., Li, C.T., Chen, Y.C., Jeng, R.J., and Dai, S.A. (2019). "Synthesis and properties of polyurea/malonamide dendritic co-adsorbents for dye-sensitized solar cells." *Polymer*, **179**, 121673.

Kay, A. and Grätzel, M. (2002). "Dye-Sensitized Core-Shell Nanocrystals: Improved Efficiency of Mesoporous Tin Oxide Electrodes Coated with a Thin Layer of an Insulating Oxide." *Chemistry of Materials*, **14**, 2930-2935.

Kusama, H. and Arakawa, H. (2013). "Influence of pyrimidine additives in electrolytic solution on dye-sensitized solar cell performance." *Journal of Photochemistry and Photobiology A: Chemistry*, **160**, 171-179.

Lee, K.M., Chen, C.Y., Wu, S.J., Chen, S.C., and Wu, C.G. (2013). "Surface passivation: The effects of CDCA co-adsorbent and dye bath solvent on the durability of dye-sensitized solar cells." *Solar Energy Materials & Solar Cells*, **108**, 70-77.

Li, J., Kong, F., Wu, G., Chen, W., Guo, F., Zhang, B., Yao, J., Yang, S., Dai, S., and Pan, X. (2014). "Di-n-alkylphosphinic acids as coadsorbents for metal-free organic dye-sensitized solar cell." *Synthetic Metal*, **197**, 188-193.

Lim, J., Kwon, Y.S., and Park, T. (2011). "Effect of coadsorbent properties on the photovoltaic performance of dye-sensitized solar cells." *Chemical Communication*, **47**, 4147-4149.

Ling, Y., Cooper, J.K., Yang, Y., Wang, G., Munoz, L., Wang, H., Zhang, J.Z., and Li, Y. (2013). "Chemically modified titanium oxide nanostructures for dye-sensitized solar cells." *Nano Energy*, **2**, 1373-1382.

Mathews, I., King, P.J., Stafford, F., and Frizzell, R. (2016). "Performance of III-V Solar Cells as Indoor Light Energy Harvesters." *IEEE Journal of Photovoltaics*, **6**, 230-235.

Nguyen, P.T., Nguyen, V.S., Phan, T.A.P., Le, T.N.V., Le, D.M., Le, D.D., Tran, V.A., Huynh, T.V., and Lund, T. (2017). "Nicotinic acid as a new co-adsorbent in dye-sensitized solar cells." *Applied Surface Science*, **392**, 441-447.

O'Regan, B. and Grätzel, M. (1991). "A low cost, high-efficiency solar cell based on dye-sensitized colloidal TiO$_2$ films." *Nature*, 353, 737-740.

Shen, H., Lin, H., Liua, Y., Li, X., Zhang, J., Wang, N., and Li, J., (2011). "A novel diphenylphosphinic acid coadsorbent for dye-sensitized solar cell." *Electrochimica Acta*, **56**, 2092-2097.

Silva, L., Freeman, H., 2019. "Variation in hydrophobic chain length of co-adsorbents to improve dye-sensitized solar cell performance." *Physical Chemistry Chemical Physics*, **21**, 16771-16778.

Son, H., Kim, C.H., Kim, D.W., Jeong, N.C., Prasittichai, C., Luo, L., Wu, J., Farha, O.K., Wasielewski, M.R., and Hupp, J.T. (2015). "Post-Assembly Atomic Layer Deposition of Ultrathin Metal-Oxide Coatings Enhances the Performance of an Organic Dye-Sensitized Solar Cell by Suppressing Dye Aggregation." *ACS Applied Materials & Interfaces*, **7**, 5150-5159.

Song, B.J., Song, H.M., Choi, I.T., Kim, S.K., Seo, K.D., Kang, M.S., Lee, M.J., Cho, D.W., Ju, M.J., and Kim, H.K. (2011). "A Desirable Hole-Conducting Coadsorbent for Highly Efficient Dye-Sensitized Solar Cells through an Organic Redox Cascade Strategy." *Chemistry-A European Journal*, **17**, 11115-11121.

Wang, Y., Sun, P., Zhao, J., Gao, M., Yi, Q., Su, Y., Gao, L., and Zou, G. (2016). "A light-scattering co-adsorbent for performance improvement of dye-sensitized solar cells." *Electrochimica Acta*, **194**, 67-73.

Zhang, Z., Zakeeruddin, S.M., O'Regan, B.C., Humphry-Baker, R., and Grätzel, M. (2005). "Influence of 4-Guanidinobutyric Acid as Coadsorbent in Reducing Recombination in Dye-Sensitized Solar Cells." *The Journal of Physical Chemistry B*, **109**, 21818-21824.

Zhang, Z.P., Evans, N., Zakeeruddin, S.M., Humphry-Baker, R., and Grätzel, M. (2007). "Effects of ω-Guanidinoalkyl Acids as Co-adsorbents in Dye-Sensitized Solar Cells." *The Journal of Physical Chemistry C*, **111**, 398-403.